Attributing extreme precipitation in South China Pearl River Delta region to anthropogenic influences based on pseudo global warming method

[1]Rui ZHAO, [1]Chi-yung TAM and [2]S.M. LEE

[1]Earth System Science Programme, the Chinese University of Hong Kong, Hong Kong, China

[2]Hong Kong Observatory, Hong Kong, China

Author information:

Rui ZHAO, final year PhD student, email: *zhaor07@link.cuhk.edu.hk*

PRESENTED AT:

1 INTRODUCTION

- Human-contributed climate warming reached approximately 1 ℃ above pre-industrial levels, increasing at 0.2℃ per decade (IPCC AR5).

- A warmer climate can increase the tropospheric moisture amount and thus the intensity of rainfall extremes, in accordance with the Clausius-Clapeyron relationship (Trenberth et al., 2003, 2015).

- Currently, it is unclear that how human-influenced climate change affects the observed characteristics of extreme precipitation in the South China Pearl River Delta (PRD) region (21.5°N-24°N, 111.9°E-115.2°E).

2 DATA, METHOD AND MODEL

2.1 Data used

- 3-hourly Tropical Rainfall Measuring Mission (TRMM) 3B42 product, at a 0.25° × 0.25° resolution for 1998-2018 period.
- 6-hourly ERA-Interim at 0.75 ° × 0.75 ° resolution, for the same time period.

2.2 Extreme rainfall event selection

We here define extreme rainfall events as their regional-accumulated rainfall amount greater than the **95th** percentile of daily precipitation during the period of 1998-2018 over the entire PRD area, based on TRMM 3B42 data. Forty extreme rainfall cases are eventually selected for attribution analysis (Figure 1).

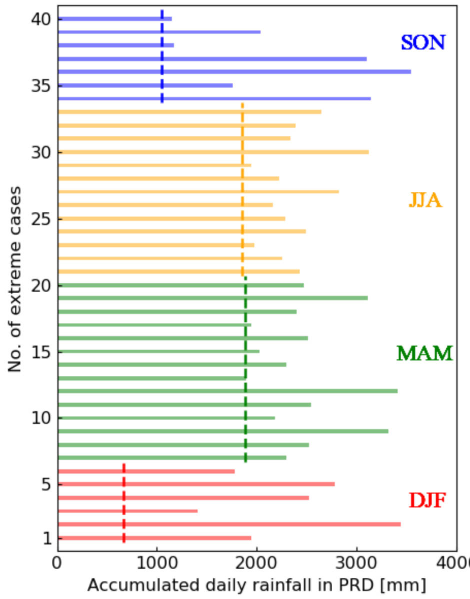

Figure 1. Accumulated rainfall amount of each extreme case that occurred in spring (MAM, green), summer (JJA, yellow), autumn (SON, blue) and winter (DJF, red) from 1998 to 2018 over the PRD region. The dashed lines denote the 95th percentile thresholds in each season.

2.3 CMIP5 GCMs selection

- To evaluate the CMIP5 model performance in predicting climate change, we compared the decadal trend of surface temperature in each model with the observed trend, such that ten GCMs with warming trend above 0.04 °C/decade are selected.
- To ensure the significance of anthropogenic warming, we selected 7 models with robust difference in time series between historical and natural runs from the ten CMIP5 models.

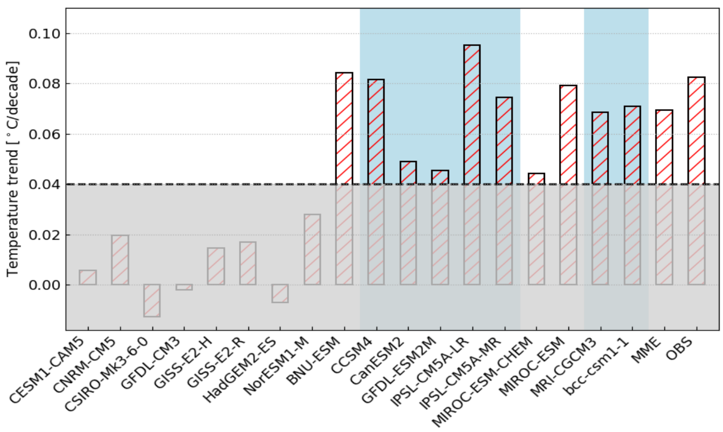

Figure 2. Surface temperature trends (°C per decade) for the period of 1901 to 2005, averaged over domain 2 (SC), derived from the historical run of individual CMIP5 models. Also shown are the ensemble mean based on selected models (highlighted by blue background) as well as observed trend.

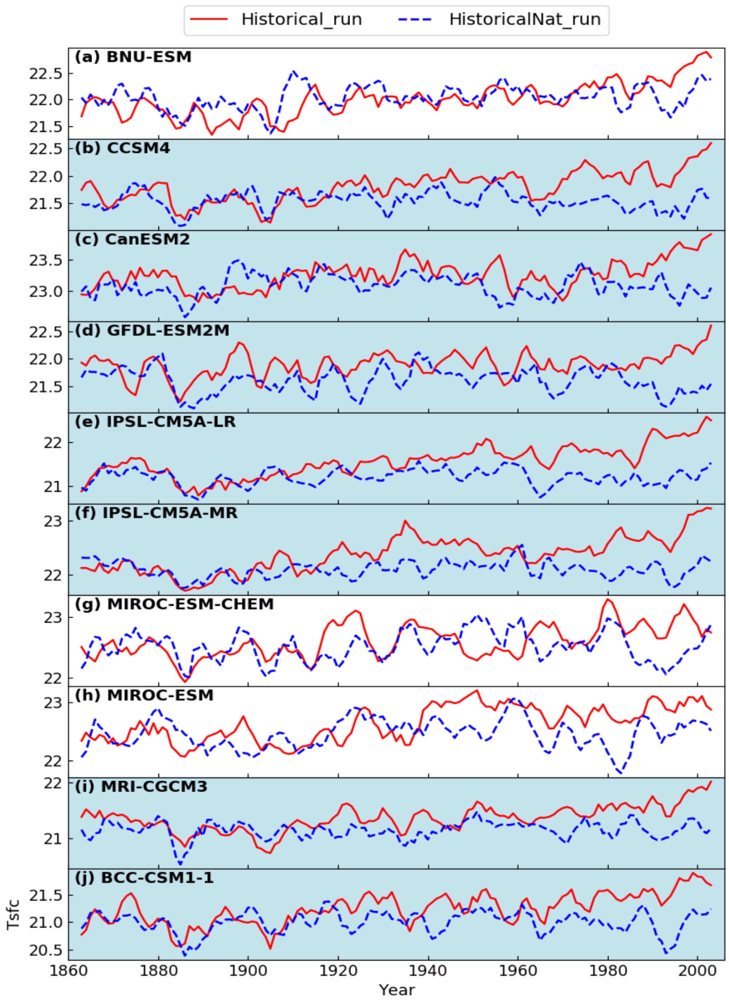

Figure 3. Time evolution of annual mean surface temperature (°C) over SC from 1861 to 2005 from the (a) BNU-ESM, (b) CCSM4, (c) CanESM2, (d) GFDL-ESM3M, (e) IPSL-CM5A-LR, (f) IPSL-CM5A-MR, (g) MIROC-ESM-CHEM, (h) MIROC-ESM, (i) MRI-CGCM3, (j) BCC-CSM1-1. Red and blue lines represent the results from historical and historicalNat runs, respectively. Models selected for obtaining anthropogenic forcing signals are highlighted by blue background.

2.4 Numerical experiments and PGW method

- Model description (WRF-ARW 3.8.1)

Table 1 WRF model settings

Domain	D01	D02 (South China)	D03 (PRD)
Resolution	50km × 50km	10km × 10km	2km × 2km
Microphysics	WSM6		
PBL physics	Bougeault-Lacarrere		

Radiation scheme	RRTMG shortwave and longwave schemes		
Land surface	Unified Noah land surface model		
Cumulus physics	Grell-3D		None
Spectral nudging	U, V-wind above 500 hPa	None	

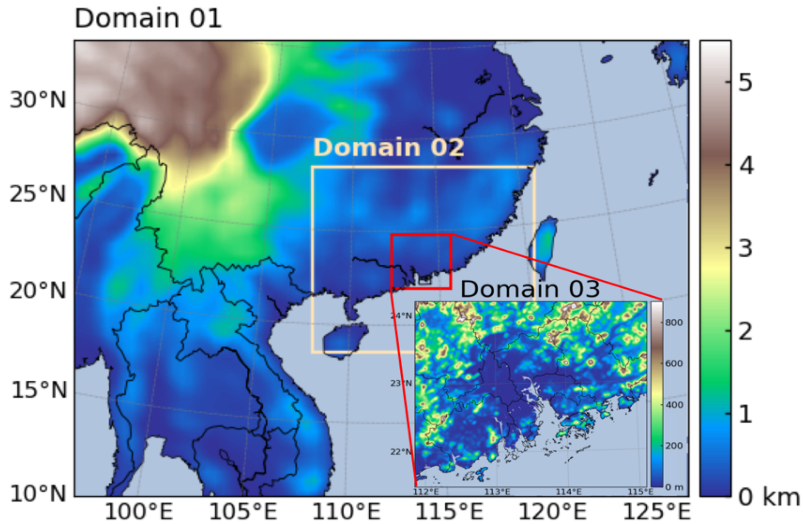

Figure 4. Spatial distribution of topography height (units: km) over the three nested domains in WRF

- Experimental design and PGW method

Two sets of experiments were carried out by downscaling the selected extreme cases in WRF, forced with 1) the initial and boundary conditions (ICBC) taken from ERA-Interim reanalysis (CTR run), and 2) counterfactual ICBC, where human influences derived from CMIP5 GCMs were removed from ERA-Interim, which is equivalent to the reversal of pseudo global warming (PGW) method (Kimura & Kitoh, 2007).

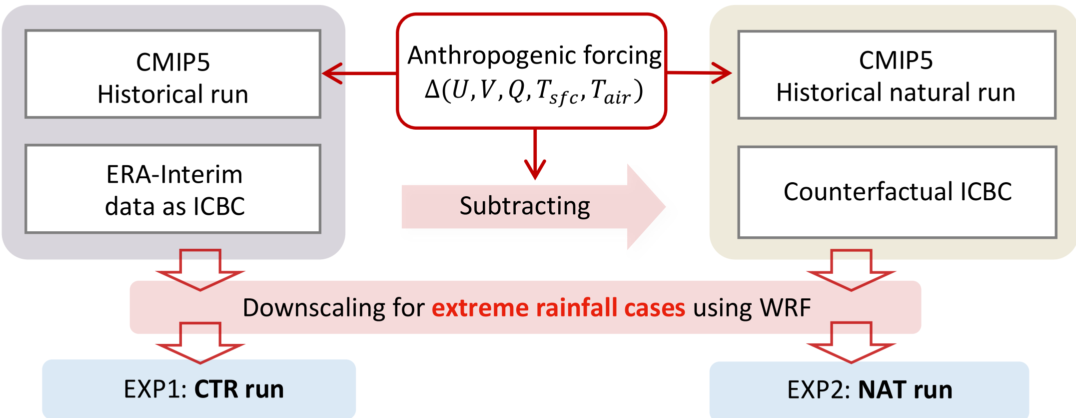

Figure 5. Schematic diagram of pseudo global warming method used in numerical experiments.

3 RESULTS

3.1 Human-induced warming

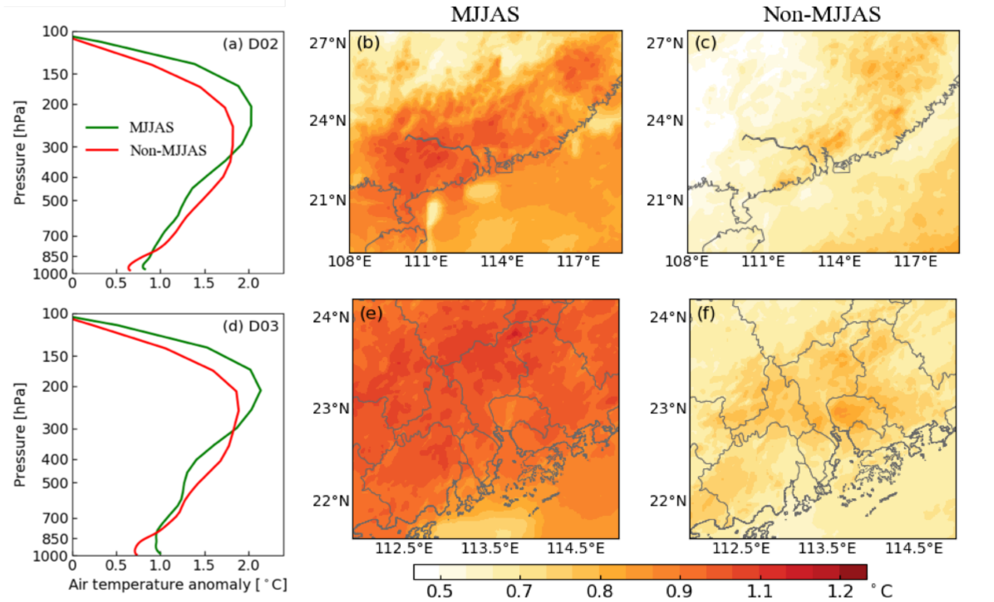

Figure 7. Difference between temperature (units: °C) from CTL and NAT runs for (a, b, c) D02 and (d, e, f) D03, during (b, e) MJJAS at 2m, and (c, f) non-MJJAS season at 2m, as well as vertical profiles of its area averaged values over the corresponding domains.

- Human-induced 1000-500hPa warming is about 0.9 (0.8) ℃ over the PRD (SC).
- Stronger warming over inland area than coastal/oceanic region.
- Vertical profiles show a larger lapse rate in non-MJJAS than MJJAS, probably due to more frequent heavy rainfall that release more latent heat and thus warm up atmosphere.

3.2 Human-induced precipitation variations

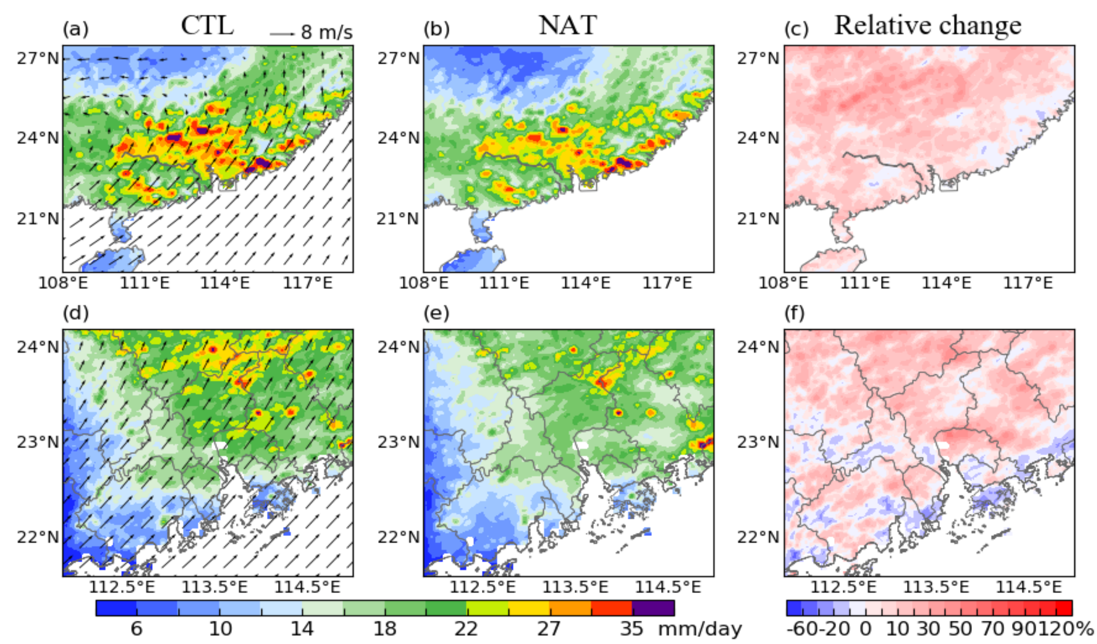

Figure 8. Daily precipitation (shading; units: mm d^{-1}) and 850-hPa winds (arrows; see scale at upper right) averaged from all the cases over (a, b, c) D02, and (d, e, f) D03 for (a, d) CTL, (b, e) NAT, as well as (e, f) the relative change between the two runs.

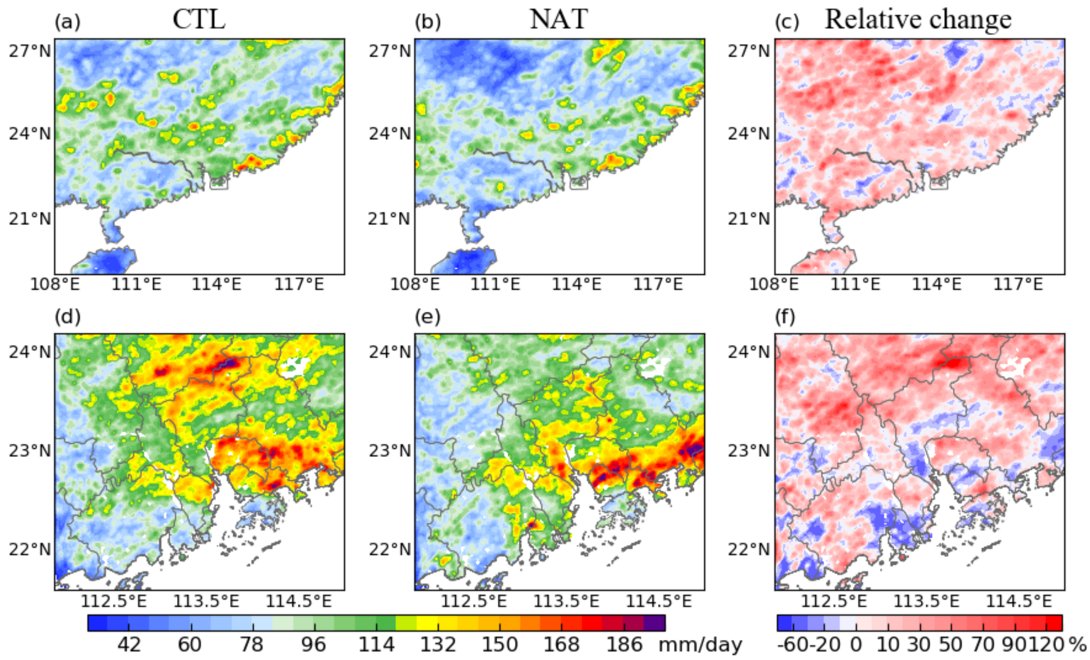

Figure 9. Same as Figure 8, but for 95th percentile of daily precipitation.

- Under anthropogenic warming, both daily mean and extreme precipitation are enhanced by at least 10% over inland while suppressed over coastal region, reflecting slightly northward shift of heaviest rainfall in CTR.
- Apparently extreme precipitation intensity increases more robust compared with daily mean rainfall.

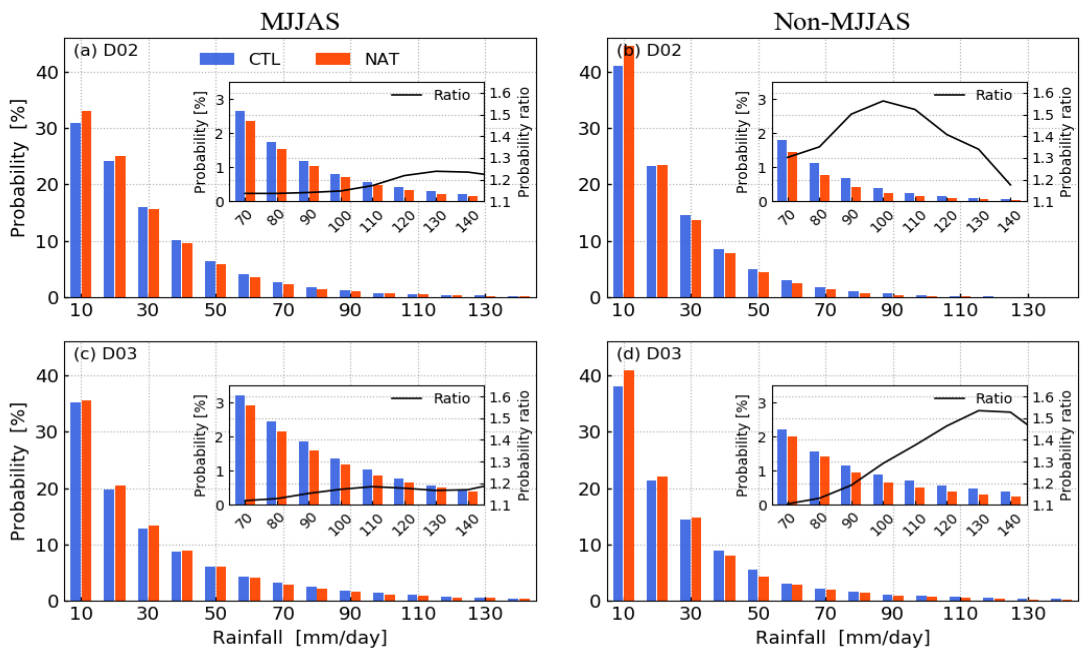

Figure 10. PDF of daily precipitation (mm d^{-1}) for CTL (blue bar) and NAT (red bar) over (a, b) SC and (c, d) PRD for cases in (a, c) MJJAS and (b, d) non-MJJAS seasons. Also shown is the ratio between probability given by CTL and NAT for rain rates greater than 70 mm per day.

- Frequency of moderate-to-extreme daily rainfall (>30 mm) enhances whereas light rainfall (<30 mm) reduces as compensate over PRD regardless of seasons.
- For heavy rainfall (> 70 mm/day), anthropogenic warming could contribute to more than 10% increase in their frequencies, with larger enhancement in non-MJJAS season over both regions.

Table 2 Human influences on precipitation and associated thermodynamic components

Variables	Types	CTR run		NAT run	
		SC	PRD	SC	PRD
2-m air temperature over land (°C)	MJJAS	25.49	27.63	24.64 (**0.8**)	26.63 (**1.0**)
	Non-MJJAS	16.25	19.60	15.61 (**0.6**)	18.87 (**0.7**)
Precipitable water (kg/m^2)	MJJAS	52.60	57.40	48.9 (**7.5%**)	54.2 (**6.0%**)
	Non-MJJAS	38.0	41.60	34.7 (**9.2%**)	38.3 (**8.6%**)
95^{th} percentile daily rainfall over land (mm)	MJJAS	73.52	86.38	69.3 (**6.1%**)	79.6 (**8.4%**)
	Non-MJJAS	57.33	75.21	52.6 (**9.0%**)	67.3(**11.7%**)

- The rate of increase in the 95^{th} percentile extreme precipitation excesses precipitable water increase for the given surface warming over PDF, which is nearly double of the CC scaling (7%/K). This super-CC increase is probably related to the wind circulation changes due to human influences. Therefore, further researches are needed to explore the possible dynamic effects in determining human-influenced extreme rainfall changes in this region.

4 CONCLUSIONS

- Low-to-mid tropospheric warming due to human activities, from 1880's to present, is about 0.8 (0.9) ℃ over the South China (PRD) region, as inferred from difference between CMIP5 historical to historical natural runs.
- Based on dynamical downscaling of heavy rain cases, extreme daily rainfall (95^{th} percentile) increased by ~8% or more, with stronger enhancement in non-MJJAS than in MJJAS season.
- Extreme precipitation intensification appears to be stronger than that in precipitable water, suggesting dynamical effects (feedback) in addition to thermodynamic effects.

This work is supported by supported by the Hong Kong Research Grants Council, General Research Fund (No. 14308017).

ABSTRACT

In the context of human-induced warming climate, greater amount of water vapor will be hold in the atmosphere, leading to more-intense precipitation extremes on global scale. However, there is no consensus yet on how much changes in those extremes are attributable to human influences on the regional basis. In this study, human-influenced variations in frequency and intensification of precipitation extremes over the South China (SC) Pearl River Delta (PRD) region are quantitatively assessed using the cloud-resolving Weather Research and Forecasting (WRF) model based on the reversed pseudo global warming (PGW) method. Forty extreme precipitation (95^{th} percentile) events that occurred in different seasons for 1998-2018 over the PRD region are identified and dynamically downscaled by the WRF. The model was forced with present and counterfactual initial and boundary conditions, with the latter being derived by subtracting the CMIP5 7-model ensemble mean changes from ERA-Interim reanalysis. As inferred from these global models, the 1000-500 hPa tropospheric temperature has warmed by ~0.9 (0.8) ℃ over PRD (SC) due to human influences. Preliminary results show that such human-induced warming can lead to about 20% or more increase in frequency of daily rainfall in PRD, with the greater enhancement in non-rainy season events. Human impacts also intensify the 95^{th} percentile of PRD daily rainfall by around 12% (8%) in non-rainy (rainy) season. This super-CC increase of non-rainy season cases probably implies the possible dynamic feedbacks, in addition to moisture-related thermodynamic effect in human-influenced extreme precipitation variations.

REFERENCE

Kimura, F., & Kitoh, A. (2007). Downscaling by Pseudo Global Warning Method. In *The Final Report of ICCAP*.

Trenberth, K. E., Dai, A., Rasmussen, R. M., & Parsons, D. B. (2003). The changing character of precipitation. In *Bulletin of the American Meteorological Society*. https://doi.org/10.1175/BAMS-84-9-1205

Trenberth, K. E., Fasullo, J. T., & Shepherd, T. G. (2015). Attribution of climate extreme events. In *Nature Climate Change*. https://doi.org/10.1038/nclimate2657